Development 130, 1439-1448

doi:10.1242/dev.00347

Induction of neuron-specific glycosylation by Tollo/Toll-8, a *Drosophila* Toll-like receptor expressed in non-neural cells

Antti Seppo, Parul Matani, Mary Sharrow and Michael Tiemeyer*

Department of Cell Biology, Yale University School of Medicine, New Haven, CT 06510, USA
*Author for correspondence (e-mail: miketiemeyer@eurofinsus.com)

Accepted 16 December 2002

SUMMARY

Specific glycan expression is an essential characteristic of developing tissues. Our molecular characterization of a mutation that abolishes neural-specific glycosylation in the *Drosophila* embryo demonstrates that cellular interactions influence glycan expression. The HRP epitope is an N-linked oligosaccharide expressed on a subset of neuronal glycoproteins. Embryos homozygous for the TM3 balancer chromosome lack neural HRP-epitope expression. Genetic and molecular mapping of the relevant locus reveals that Tollo/Toll-8, a member of the Toll-like receptor family, is altered on the TM3 chromosome. In wild-type embryos, Tollo/Toll-8 is expressed by ectodermal cells that surround differentiating neurons and precedes HRP-epitope appearance. Re-introduction of Tollo/Toll-8 into null embryos rescues neural-specific glycan expression. Thus, loss of an ectodermal cell surface protein alters glycosylation in juxtaposed differentiating neurons. The portfolio of expressed oligosaccharides in a cell reflects its identity and also influences its interactions with other cells and with pathogens. Therefore, the ability to induce specific glycan expression complements the previously identified developmental and innate immune functions of Toll-like receptors.

Key words: Toll-like receptor, Glycosylation, HRP epitope, N-linked oligosaccharide, Neuronal differentiation

INTRODUCTION

Eukaryotic cells are enveloped within a complex coating of carbohydrate. Composed of the pendant oligosaccharide moieties of glycoproteins, glycolipids and proteoglycans, the glycocalyx constitutes the interface at which cells interact with each other and with their environment. Glycans mediate cellular recognition and adhesion, facilitate protein maturation, regulate protein activity through allostery and bioavailability, influence receptor ligation, and modulate transmembrane signaling (Varki, 1993; Hammond et al., 1994; Tsuda et al., 1999; Sharrow and Tiemeyer, 2001; Moloney et al., 2000; Vyas et al., 2002). Specific oligosaccharide structural elements participate in each of these processes, requiring spatial and temporal regulation of glycan synthesis in developing and mature organisms. As a consequence of regulated expression, oligosaccharide structures are among the most discriminating markers for cellular differentiation in complex tissues (Feizi, 1985; Dodd and Jessell, 1985; Allendoerfer et al., 1999; Matthews et al., 2002). Despite extensive descriptions of specific oligosaccharide distributions, the cellular and molecular mechanisms by which cells achieve expression of their characteristic portfolio of surface glycans are largely unknown.

Antibodies raised against the plant glycoprotein, Horseradish Peroxidase (HRP), crossreact with an N-linked oligosaccharide epitope that is distributed throughout the *Drosophila melanogaster* nervous system and is also expressed in a small, well characterized subset of non-neural tissues (Jan and Jan, 1982; Snow et al., 1987). Two mutations abolish expression of the HRP epitope. In the first, designated *nac*, the epitope is absent in the larval, pupal and adult nervous system (Katz et al., 1988). The molecular nature of the *nac* mutation is unknown, but affected adults exhibit sensory afferent defasciculation and behavioral phenotypes (Whitlock, 1993; Phillis et al., 1993). The second mutation that abolishes HRP-epitope expression is carried on the TM3 balancer chromosome, an extensively rearranged form of the third chromosome (Snow et al., 1987). TM3 homozygotes do not express the HRP epitope in the embryonic nervous system but do produce the glycan in the expected non-neural tissues. Therefore, it is likely that the structural genes necessary for synthesis of the HRP epitope are intact and that the TM3 mutation alters a gene that regulates tissue-specific glycosylation.

We report characterization of the TM3 locus that abolishes HRP-epitope expression. The affected gene, which we named '*tollo*' encodes a member of the family of cell surface receptors with homology to the Toll protein (Toll-like receptors, TLRs). Genome sequence characterization re-identified the tollo locus, resulting in its designation as '*toll-8*' (Tauszig et al., 2000). The founding member of the TLR family (Toll) was originally identified as a component of the signaling pathway that induces dorsal-ventral polarity in the *Drosophila* embryo (Anderson et al., 1985). Subsequently, TLRs have also been shown to participate in innate immune responses in *Drosophila* and other

organisms by transducing pattern recognition signals (Hoffman et al., 1999; Medzhitov et al., 1997; Williams et al., 1997; Ip and Levine, 1994). We now add the induction of tissue-specific glycosylation to the list of TLR functions.

MATERIALS AND METHODS

Reagents

Rabbit antiserum against HRP (anti-HRP antibody) and secondary antibodies were obtained from Jackson Laboratories (Westgrove, PA). Monoclonal antibodies 1D4, BP102 and 22C10 were provided by Corey Goodman, University of California at Berkeley. Genomic clones in P1 phage were obtained from the Artavanis-Tsakonas laboratory and grown using standard methods.

Fly stocks and deletion screens

A non-complementation screen using the third chromosome deletion set (Bloomington Stock Center) was performed to determine which region of the TM3 balancer chromosome is responsible for loss of the HRP epitope. For deletion stocks maintained over the TM3 balancer, embryos were collected and stained for loss of the HRP epitope. For stocks not already over the TM3 balancer, progeny were collected from a cross of the deletion stock to a TM3 stock in which the balancer carried an embryonically expressed *lacZ* marker (*D*, *ry*/TM3-DZ, P{ry+t$^{7.2}$=H22.7}, Bloomington Stock Center). The *lacZ* activity, detectable in maxillary segments from stage 12-17, allowed the HRP-status of blue embryos to be interpreted as complementation/non-complementation of the TM3 mutation.

Once a region of interest was identified (by the *fz*^{M21} interval 70D2/3-71E4/5), additional deletions were obtained to refine the location of the affected TM3 locus. Deletion lines and their breakpoints from sources other than the Bloomington Stock Center were as follows: *D*^{5rv14} (70D1/2-71C1/2; A. Carpenter, University of Cambridge), *Brd*^{15} (71A1/2-71C1/2; J. Posakony, University of California at San Diego) and *fz*^{D21} (70D2-70E8, Umeå Stock Center). Other deletions were obtained from the Bloomington Stock Center: Df(3L)BK10 (71C3 – 71E5), *D*^{5rv5} (70C3/4 – 70F5/71A1), *fz*^{GS1a} (70D1 – 70E7) and *fz*^{GF3b} (70C1/2 – 70D4/5). The Gal4 driver stocks, *rhomboid*-Gal4, *ELAV*-Gal4 and *hsp70*-Gal4 were obtained from Tian Xu and a second chromosome UAS-*lacZ* line was obtained from Haig Keshishian (both at Yale University).

Immunohistochemistry, lacZ activity staining and in situ hybridization

Embryo collections were dechorionated, fixed, devitellinized, stained with antibodies and staged according to standard methods (Patel, 1994; Campos-Ortega and Hartenstein, 1985). Primary antibody dilutions were 1:500 for rabbit anti-HRP, 1:3 for BP102, 1:5 for 22C10 and 1:10 for 1D4. lacZ activity was detected in embryos as previously described (Klämbt et al., 1991). The distribution of *tollo* mRNA in embryos was visualized by in situ hybridization using single-stranded DNA probes labeled with digoxigenin (Tautz and Pfeifle, 1989). For co-localization of *tollo* mRNA and mAb 22C10 staining, in situ hybridization was performed first, using digoxigenin-11-UTP-labeled RNA probes prepared by in vitro transcription (Kopczynski et al., 1996). For RNA and DNA probes, a 2.4 kb EcoR1 genomic fragment (*tollo* nucleotide 2796 to 5230) served as template. Embryos were routinely examined with sense and antisense probes prepared from plasmid templates bearing insert in opposite orientations.

Reverse northern analysis, sequence assembly and genomic characterization

Poly-A$^+$ RNA was isolated from OreR or *Brd*^{15}/TM3 embryonic total RNA by hybridization to biotinylated poly-dT oligonucleotide followed by capture and release from streptavidin magnetic beads as recommended by the manufacturer (Boehringer/Roche). To generate probe for Reverse Northern analysis, poly-A$^+$ mRNA was dephosphorylated with calf intestinal phosphatase and then end-labeled with γ-^{32}P-ATP by T4 Polynucleotide Kinase (Sambrook et al., 1989). Drosophila genomic DNA in P1 phage was digested with restriction enzymes, electrophoresed, transferred to nylon and probed with end-labeled mRNA prepared from OreR or *Brd*^{15}/TM3 embryos.

A 2.4 kb *Eco*RI fragment that demonstrated differential hybridization was isolated from P1 phage DS06206, subcloned into pBluescript (Stratagene) and sequenced in both directions by multiple rounds of overlapping sequence acquisition with the dideoxy chain termination method (W. M. Keck, Biotechnology Resource Center at Yale University). The open-reading frame (ORF) identified in the *Eco*RI fragment was extended in the 5′ direction by overlapping sequencing reactions that used DNA isolated from P1 phage DS06206 as template. The resulting genomic DNA sequence, containing a 4038 nucleotide ORF, 17 nucleotides of 5′-, and 1189 nucleotides of 3′-UTR, was submitted to GenBank (Accession Number, AF204158).

Sequence was extended in the 3′ direction by 3′-RACE (Clontech Marathon) with poly-A$^+$ RNA isolated from OreR or *Brd*^{15}/TM3 embryos and nested primer sets (Frohman, 1993). Distinct bands of 1.6 kb from OreR and 1.2 kb from *Brd*^{15}/TM3 were obtained. Primer design incorporated restriction sites (5′ *Pst*I and 3′ *Xho*I) for ease of subcloning. The final 3′-RACE reactions were digested with *Pst*I and *Xho*I, yielding fragments (1.1 kb from OreR and 0.9 kb from *Brd*^{15}/TM3) that were subcloned into pBluescript and sequenced. Promoter components were identified by the NNPP2.1 prediction tool (Berkeley *Drosophila* Genome Project). Other sequence analysis used BLAST programs available through the National Center for Biotechnology Information (Altschul et al., 1997). Northern analysis used poly-A$^+$ RNA isolated from overnight embryo collections and genomic Southern analysis used genomic DNA prepared from adults. Both blotting procedures were performed by standard methods using random-primed ^{32}P-labeled DNA probes (Sambrook et al., 1989).

Generation of rescue constructs and transformant lines

Plasmid bearing a full-length *tollo* insert was constructed with DNA from two overlapping *Drosophila* genomic clones in P1 phage. The 2.4 kb *Eco*RI fragment isolated from P1 clone DS06206, containing 3′ tollo sequence, was ligated into the *Eco*RI site of pBluescript I (KS)+. The resulting plasmid was digested with *Sal*I (cuts in the 5′ polylinker) and *Mlu*I (cuts in *tollo* 3′-UTR) to accept a 7.5 kb *Sal*I/*Mlu*I fragment prepared from P1 clone DS05329. In addition to a complete *tollo* ORF, the resulting plasmid (designated pG*tollo*) contains 2.5 kb of 5′ and 1.2 kb of 3′ genomic sequence.

To generate a rescue construct in which *tollo* coding sequence was placed under control of UAS elements, a *Not*I site was introduced into the full-length *tollo* construct (pG*tollo*) by PCR such that the enzyme cut 11 nucleotides upstream from the first ATG codon. *Not*I digest of the resulting construct, designated pG*tollo*N$_{-11}$, released a 5.2 kb fragment that was ligated into *Not*I-linearized pUAST transformation vector to produce pUAST*tollo* (Brand et al., 1994).

To generate a transformation construct in which Gal4 expression was controlled by *tollo* 5′ genomic sequence, a *Not*I site was introduced into cloned genomic DNA by PCR (pG*tollo* template) such that the enzyme cut seven nucleotides upstream from the first ATG codon. The amplified fragment was subcloned into pCR2.1 and recovered as a 2.5 kb fragment with a 5′ blunted *Sal*I end and a 3′ *Not*I end. After ligation into the pCaSpeR3 transformation vector (previously digested with *Stu*I/*Not*I), Gal4 coding sequence was added as a *Not*I fragment, prepared from pGaTN, to yield a construct designated p*tollo*Gal4 (Brand and Perrimon, 1993).

Transformant lines were produced by injection of rescue constructs into *w*^{1118}; *Sb*,Δ2-3/TM6b flies by standard procedures. Transformation with the pUAST*tollo* or p*tollo*Gal4 vector yielded

insertions on both the X and second chromosomes that were then crossed into the *Brd*^{15}/TM3-*lacZ* background.

RESULTS

An aberration on the TM3 balancer chromosome that abolishes HRP-epitope expression maps to 71C1/2

Embryos homozygous for the TM3 balancer chromosome fail to express the HRP epitope in the ventral nerve cord and peripheral nervous system, although expression is maintained in three non-neural tissues (Fig. 1A,B). TM3 rearrangement breakpoints provide likely candidates for regions of the third chromosome that affect HRP-epitope expression. To assess the relevance of these breakpoints and to ensure that a gene located between TM3 breakpoints was not missed, overlapping deletion stocks that together cover approximately 80% of the third chromosome were screened for their ability to complement loss of the HRP epitope in a TM3 background (Fig. 2). The smallest non-complementing deletion (Fig. 1C, breakpoints 71A1/2-71C1/2) is carried in a *Bearded* stock designated *Brd*^{15} (Leviten and Posakony, 1996). The combination *Brd*^{15}/TM3 or *Brd*^{15}/TM3-*lacZ* produces viable and fertile adults.

Of the relevant genotypes, only *Brd*^{15} homozygotes display gross morphologic aberrations (Fig. 1D-G). *Brd*^{15}/*Brd*^{15} embryos develop normally until stage 14 when defects in the formation of anterior terminal structures become apparent. In particular, retraction of the clypeolabrum is stalled in *Brd*^{15} homozygotes, causing the supraesophageal ganglia (embryonic brain lobes) to appear exteriorized. The head involution defect provides an unambiguous, reliable diagnostic for the *Brd*^{15} homozygous genotype (Fig. 1G, arrowhead). Examination of neural tissue integrity by monoclonal antibody staining demonstrates that longitudinal and commissural bundles are present in the central nervous system (mAb BP102), appropriate cell numbers and approximate cellular relations are preserved in the peripheral nervous system (mAb 22C10), and efferent motor pathways develop normally (mAb 1D4) in *Brd*^{15} homozygotes. Thus, neural differentiation and axon extension, to the extent that they are revealed by these mAb markers, are unaffected by *Brd*^{15}.

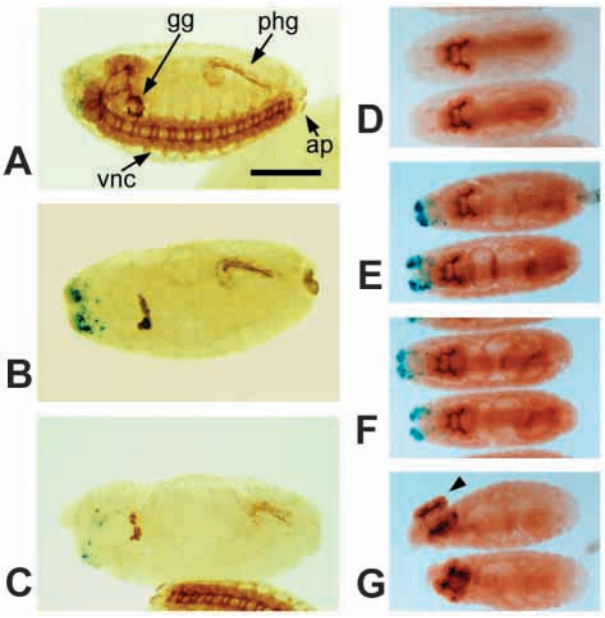

Fig. 1. A third chromosome deletion uncovers an aberration on the TM3 balancer that is responsible for loss of the HRP epitope. (A) In balanced wild-type embryos (+/TM3-*lacZ*), anti-HRP antibodies stain the central nervous system (vnc, ventral nerve cord) and the peripheral nervous system (out of the plane of focus). Three non-neural tissues also express the HRP epitope: the garland gland (gg), anal pads (ap) and the posterior hindgut (phg). Blue staining at the anterior end of the embryo (towards the left in all panels) indicates the relative dose of the TM3-*lacZ* chromosome. (B) In TM3 homozygotes, the HRP epitope is absent from the nervous system but still detected in non-neural tissues. (C) *Brd*^{15} fails to complement the TM3 defect (*Brd*^{15}/TM3-*lacZ*) and the epitope is still detected in non-neural tissues. (D-G) Whole-mount embryos were double stained: first for *lacZ* activity to confirm genotype; and then with mAb BP102 to provide landmarks for comparison of embryonic gross morphology. Dorsal views of stage 15 and 16 embryo pairs are shown for the genotypes (D) +/+, (E) TM3-*lacZ*/TM3-*lacZ*, (F) *Brd*^{15}/TM3-*lacZ* and (G) *Brd*^{15}/*Brd*^{15}. *Brd*^{15} homozygotes display a characteristic defect in head involution (arrowhead in G). Scale bar: 350 μm in A-C; 500 μm in D-G.

Reverse-Northern analysis identifies a message that is differentially expressed in wild-type and *Brd*^{15}/*TM3* embryos

The proximal breakpoint of the *Brd*^{15} deletion (71C1/2) overlaps a TM3 rearrangement breakpoint at 71C (Lindsley and Zimm, 1992). Therefore, P1 phage clones that map to the 71C1/2 interval were obtained and probed with ^{32}P-end-labeled mRNA prepared from embryo collections from OreR or *Brd*^{15}/TM3 stocks. The P1 phage clone designated DS06206 contains a 2.4 kb *Eco*RI fragment and a 1.1 kb *Bam*HI/*Xba*I fragment that are both transcribed in OreR but not detected in *Brd*^{15}/TM3 embryos (Fig. 3A-C). Subsequent sequence

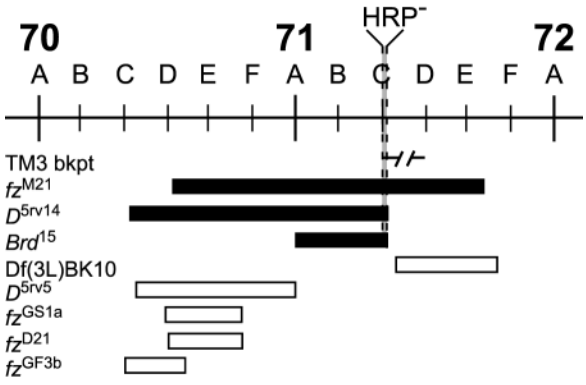

Fig. 2. Deletion non-complementation maps loss of the HRP epitope to a TM3 breakpoint at 71C. Deletions covering the third chromosome were screened for loss of the HRP epitope in combination with the TM3 balancer. Breakpoints are indicated for complementing deletions (white) and non-complementing deletions (black). The gray zone labeled HRP$^-$ indicates the smallest region that contains a gene responsible for HRP-epitope expression. The distal end of the interval is defined by the TM3 breakpoint at 71C. The proximal breakpoint is limited to 71C1/2 by *D*^{5rv14} and *Brd*^{15}.

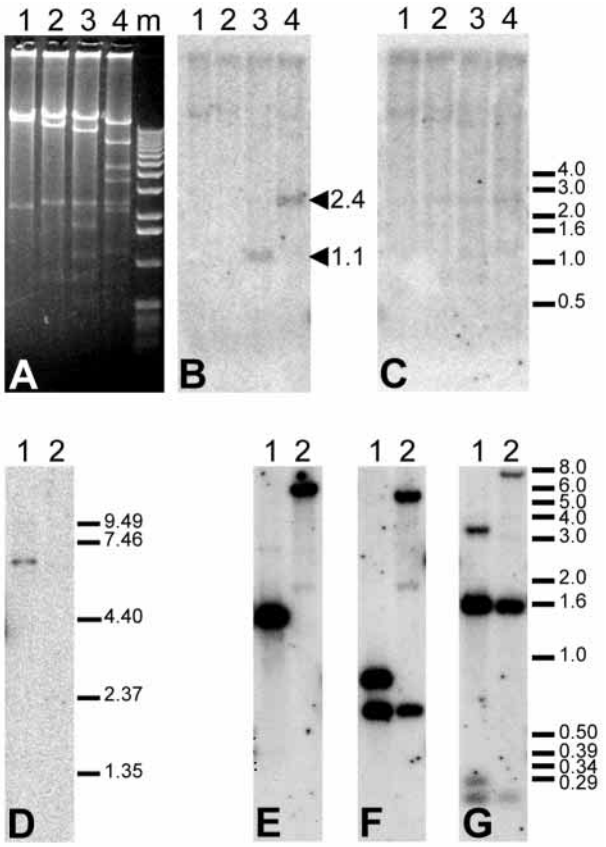

Fig. 3. A differentially expressed transcript and genomic polymorphisms distinguish *Brd*^{15}/TM3 from OreR embryos. (A-C) Reverse-northern analysis. DNA from P1 phage DS06206 was digested with *Bam*HI (lane 1), *Xba*I (lane 2), *Bam*HI/*Xba*I (lane 3) or *Eco*RI (lane 4) then electrophoresed (m indicates marker lane, 1 kb ladder). (A) Ethidium bromide staining of agarose gel. Blots prepared from the gel were probed with ^{32}P-end-labeled mRNA isolated from OreR (B) or from *Brd*^{15}/TM3 embryos (C). A differentially expressed 2.4 kb *Eco*RI band was subcloned. (D) Northern analysis. Poly-A$^+$ RNA isolated from OreR (lane 1) or *Brd*^{15}/TM3 embryos (lane 2) was probed with the 2.4 kb *Eco*RI fragment. (E-G) Southern analysis. Genomic DNA prepared from OreR (lane 1) or from *Brd*^{15}/TM3 (lane 2) adults was digested with (E) *Hin*dIII, (F) *Hin*dIII/*Xba*I or (G) *Pst*I and probed with a 1.5 kb *Hin*dIII fragment (see Fig. 4 for restriction map and probe locations). Digestion with *Pst*I produces the smallest polymorphic fragment, a 280 bp fragment in OreR that is shifted to ~7.5 kb in *Brd*^{15}/TM3.

analysis placed the 1.1 kb fragment within the 2.4 kb fragment. Probe prepared from the 2.4 kb *Eco*RI fragment was used to probe northern blots of poly-A$^+$ RNA isolated from OreR or *Brd*^{15}/TM3 embryos. A 6.5-7.0 kb band was identified in the OreR preparation that was not detected in *Brd*^{15}/TM3 poly-A$^+$ RNA (Fig. 3D). Genomic Southern analysis demonstrates multiple restriction fragment length polymorphisms in the *Brd*^{15}/TM3 genotype. Probe prepared from the 2.4 kb *Eco*RI fragment hybridizes to a 1.5 kb *Hin*dIII fragment in OreR that is shifted to approximately 6 kb in *Brd*^{15}/TM3. In turn, probe prepared from the 1.5 kb *Hin*dIII fragment identifies the same polymorphism as well as 876 bp *Hin*dIII/*Xba1* and 280 bp *Pst*I fragments that also differentiate the two genotypes (Fig. 3E-G).

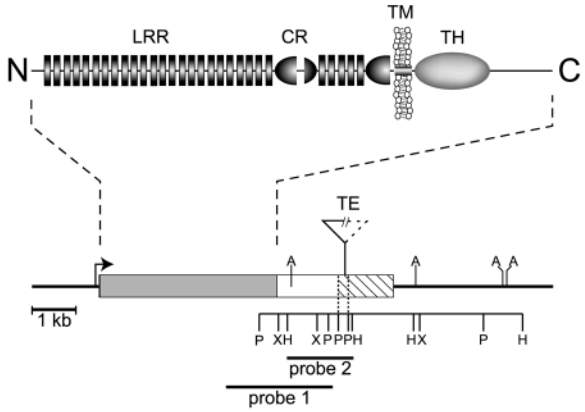

Fig. 4. The disrupted gene in *Brd*^{15}/TM3 embryos encodes a Toll-like receptor. The wild-type *tollo* gene predicts a protein of 1346 amino acids. (Top) Conserved sequence domains identify the gene as a Toll-like Receptor (black rectangles, leucine-rich repeats, LRR; discontinuous black ovals, cysteine-rich domains, CR; gray oval, Toll homology signaling domain, TH; putative transmembrane domain, TM). (Bottom) Genomic sequence (nucleotides 17001 to 30000 from AE003531) contains a 4038 nucleotide ORF (gray box) within a single exon. Nucleotide 1 in the *tollo* ORF corresponds to nucleotide 18564 in AE003531. The boxed region (6735 nucleotides) was sequenced, either from genomic DNA derived from P1 phage (gray and white, nucleotides –17 to 5717) or by overlapping 3′-RACE (hatched, nucleotides 5398 to 6718). Arrow at the 5′ end indicates a predicted promoter. Four consensus polyadenylation signals (A) are found within 5 kb of the first in-frame stop codon. Sequence divergence in the TM3 chromosome is indicated by a broken line transposable element (TE). A polymorphic *Pst*I genomic fragment confirms the site of divergence and is indicated in the aligned restriction map for the region (P, *Pst*I; X, *Xba*I; H, *Hin*dIII). Probe 1 (*Eco*RI fragment) used for in situ hybridization and northern blots. Probe 2 (*Hin*dIII fragment) used for genomic Southern analysis.

The differentially transcribed *Drosophila* genomic fragment contains a Toll-like receptor gene

The sequenced 2.4 kb *Eco*RI genomic fragment yielded an open reading frame of 1250 bp which was extended to 4038 bp in length by further genomic sequencing (Fig. 4). Motifs in the predicted protein define it as a member of the Toll-like Receptor family (Hashimoto et al., 1988). Leucine-rich repeats and cysteine-rich domains are found in the extracellular portion of the molecule and a Toll homology (TH) domain is present in the C-terminal region. Based on the TH similarity and on the inability of *Brd*^{15}/TM3 adults to reliably extricate themselves from their food, we named the gene ‘tollo’, a Finnish word roughly translated as ‘stupid’.

A total of 6735 nucleotides were sequenced, extending from 17 bp upstream of the ORF to 2677 bp beyond the first in-frame stop codon, and found to be co-linear with genomic sequence in GenBank Accession Number AE003531 and with *Drosophila* cDNA sequence LD 33590 (Adams et al., 2000; Rubin et al., 2000). The sequence predicts that the *Hin*dIII, *Xba*I and *Pst*I polymorphisms observed in *Brd*^{15}/TM3 lie in the 3′ UTR of the gene (Fig. 3E-G). To more precisely define the polymorphism, 3′-RACE was performed on poly-A$^+$ RNA isolated from OreR and *Brd*^{15}/TM3 embryos. The fragment

amplified from *Brd*^{15}/TM3 embryos yielded 969 nucleotides of sequence of which the first 237 matched previously sequenced genomic DNA. However, TM3 sequence diverged from wild-type at a position corresponding to nucleotide 5635, 1.6 kb downstream from the first in-frame stop codon of *tollo* (nucleotide 4039) and within the 3′ UTR predicted by mRNA size (Fig. 3D, Fig. 4). Sequence obtained for the first 732 bases of divergence matches a *Drosophila* transposable element designated '412', GenBank Accession Number X04132 (Yuki et al., 1986). It was not determined whether the divergent sequence reflects the insertion of an intact transposable element or identifies the site of the TM3 rearrangement breakpoint previously mapped to 71C.

Tollo mRNA is expressed in non-neural ectodermal cells that contact neural precursor cells

Expression of *tollo* mRNA is first detected in the cellular blastoderm, initially as prominent bands at both ends of the embryo (Fig. 5A). Very rapidly, *tollo* mRNA appears in dorsoventral bands repeated along the entire length of the embryo (Fig. 5B). As germband retraction begins, late in stage 12, the bands of *tollo* mRNA span the entire width of the germband (Fig. 5C,D), placing Tollo expression within ectodermal domains from which ventral nerve cord precursor cells differentiate and delaminate. By the time germband retraction is complete (stage 13), *tollo* mRNA expression disappears from the ventral ectoderm that underlies the delaminated, discrete nerve cord. Expression of the HRP epitope in the ventral nerve cord is first detected reproducibly at stage 14, shortly after *tollo* mRNA decreases. Thus, Tollo expression in ventral ectoderm coincides with a period of maximal contact with differentiating neurons and disappears once neurons segregate from the ectoderm to form a consolidated ventral nerve cord.

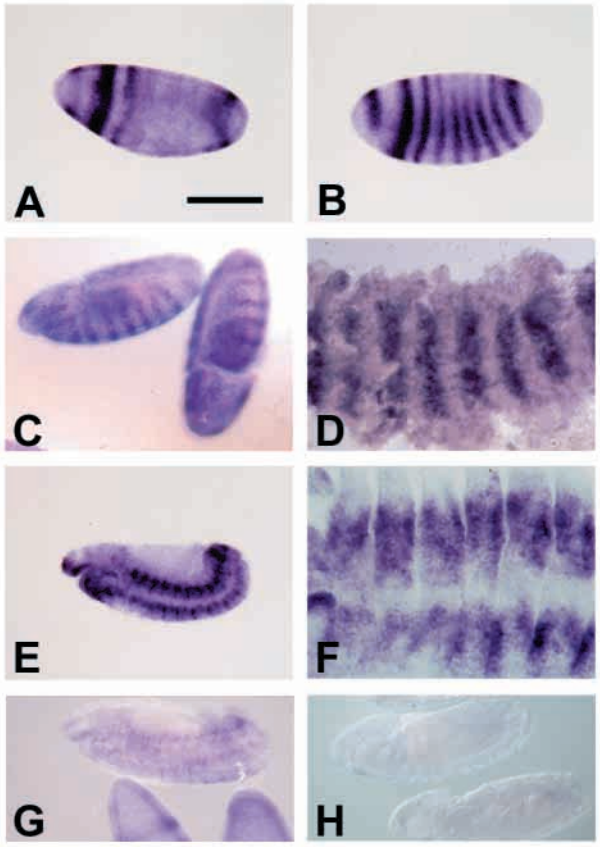

Fig. 5. *Tollo* mRNA is dynamically expressed throughout embryogenesis. The distribution of *tollo* mRNA was visualized by in situ hybridization with digoxigenin-labeled probes in OreR (A-F), TM3/TM3 (G) and *Brd*^{15}/*Brd*^{15} (H) embryos. Message is first detected in distinct anterior and posterior bands at the cellular blastoderm stage (A) but rapidly spreads to include bands along the entire length of the embryo (B). At stage 12 (C,D), the extended germ-band demonstrates segmental expression. By stage 13 (E) ectodermal expression is restricted to domains within each segment. At higher magnification (F), stage 13 expression of *tollo* mRNA is not uniform within lateral ectodermal domains. TM3 homozygotes (G, stage 13) exhibit weak hybridization signal, while *Brd*^{15} homozygotes (H, stage 14) completely lack message. Scale bar: 450 μm in A-C,E,G,H; 125 μm in D,F.

In the lateral ectoderm, *tollo* mRNA is found in distinct, segmentally repeated domains at stage 13. Together, these repeated domains form continuous anteroposterior stripes of ectodermal expression (Fig. 5E,F). Within each domain, expression is not uniform. Cells at the segment boundaries express higher levels of *tollo* mRNA, forming ectodermal pockets that are partly lined with Tollo-expressing cells. By early stage 15, *tollo* mRNA is greatly reduced in the lateral ectoderm and expressing domains are attenuated to a few cells immediately adjacent to segment boundaries. Expression of the HRP epitope in the peripheral nervous system is first detected reproducibly at stage 15, shortly after *tollo* mRNA expression has decreased in the lateral ectoderm.

Consistent with the determination that the TM3 chromosome has not lost the entire *tollo* gene (Figs 3, 4), hybridization signal was detected in TM3/TM3 embryos (Fig. 5G). Thus, RNA that contains *tollo* sequence is produced in TM3 embryos despite being undetectable in blotted poly-A$^+$ mRNA preparations (Fig. 3D). Hybridization to *Brd*^{15}/*Brd*^{15} embryos was not detected at any stage, indicating that the anti-sense probe is specific for *tollo* and does not cross-hybridize to other embryonically expressed Toll-like receptors (Fig. 5H).

The position of Tollo-expressing domains along the dorsoventral axis of the lateral ectoderm closely approximates the site of proneural cluster formation (Blochinger et al., 1990). Therefore, *tollo* mRNA expression was localized relative to the position of differentiating neurons in the peripheral nervous system (Fig. 6A,B). Within the lateral domains of Tollo expression found in each segment, maturing neurons occupy patches that display reduced or undetectable *tollo* mRNA (Fig. 6A). At stage 14, all but the earliest neurons to differentiate (which have actively begun to migrate away from their birthplace towards their final embryonic positions) are found in close association with ectodermal cells that express *tollo* mRNA (Fig. 6B). Thus, in the peripheral nervous system, as in the ventral nerve cord, Tollo expression coincides temporally with periods of neural differentiation that are characterized by maximal contact between the ectoderm and neural precursor cells.

Transgenic expression of Tollo rescues expression of the HRP epitope

To determine whether *tollo* is sufficient to rescue expression of

the HRP epitope in the *Brd*^{15} homozygote, a transformation construct was generated (pUAST*tollo*) that placed *tollo*-coding sequence under the control of UAS elements (Brand et al., 1994). A second transformation construct was prepared (p*tollo*Gal4) that placed Gal4 expression under control of 2.5 kb of *Drosophila* genomic DNA found immediately upstream of the *tollo* initiation codon (Brand and Perrimon, 1993). *Tollo*-Gal4 transformant lines were crossed to a UAS-*lacZ* reporter line and embryo collections were stained for β-galactosidase activity. Both in the germband extended embryo at stage 12 (Fig. 7A,B) and in the lateral ectoderm of the stage 13 embryo (Fig. 7C,D), *lacZ* activity matched the distribution of *tollo* mRNA detected by in situ hybridization. Thus, the 2.5 kb of genomic DNA incorporated into the p*tollo*Gal4 transformation vector contains control sequences sufficient to recapitulate normal Tollo expression.

UAS-*tollo* and *tollo*-Gal4 transformant lines were separately prepared in the *Brd*^{15}/TM3 background. HRP-epitope expression is absent from embryos collected from lines bearing either construct alone. However, when UAS-*tollo* and *tollo*-Gal4 lines are crossed to each other, HRP-epitope expression is rescued in embryos that lack (*Brd*^{15}/TM3 and TM3/TM3 genotypes) and in embryos that possess (*Brd*^{15}/*Brd*^{15}) the head involution defect associated with the *Brd*^{15} deletion (Fig. 8A,D,G, see arrowhead). Thus, the head involution defect is independent of HRP-epitope expression. *Tollo*-Gal4/UAS-*tollo* rescues HRP-epitope expression in the ventral nerve cord (Fig. 8B,E,H) and in the peripheral nervous system (Fig. 8C,F,I).

Other Gal4 driver lines were screened for their ability to rescue the HRP epitope in UAS-*tollo* transformants. Neither a pan-neural driver (*ELAV*-Gal4) nor a mesectodermal/midline glial driver (*rhomboid*-Gal4) rescued oligosaccharide expression when crossed to UAS-*tollo*, despite their ability to drive expression in cells that make extensive contact with neuronal surfaces. Therefore, simple juxtaposition of Tollo protein and a neuron is insufficient; induction of the neuronal HRP epitope requires Tollo expression in appropriate non-neural ectodermal cells.

Heat-shock driven expression of Tollo in all cells (*hsp70*-Gal4/UAS-*tollo*) generates early embryonic lethality that precludes assessment of HRP-epitope rescue. However, in the course of these experiments, *hsp70*-Gal4/UAS-*tollo* embryos not subjected to heat shock were also collected and stained with anti-HRP antibody. Unexpectedly, unshocked embryos older than stage 15 express the HRP epitope in the salivary gland and in sensory neurons most proximal to the gland (Fig. 8J,K). Other neuronal populations were not stained, whether in the CNS or in more posterior segments of the PNS. Thus, leaky Gal4 expression in the salivary gland (verified by UAS-*lacZ* reporter) is sufficient to induce the HRP epitope in a tissue that does not normally express the glycan and is able to rescue the epitope in nearby sensory neurons.

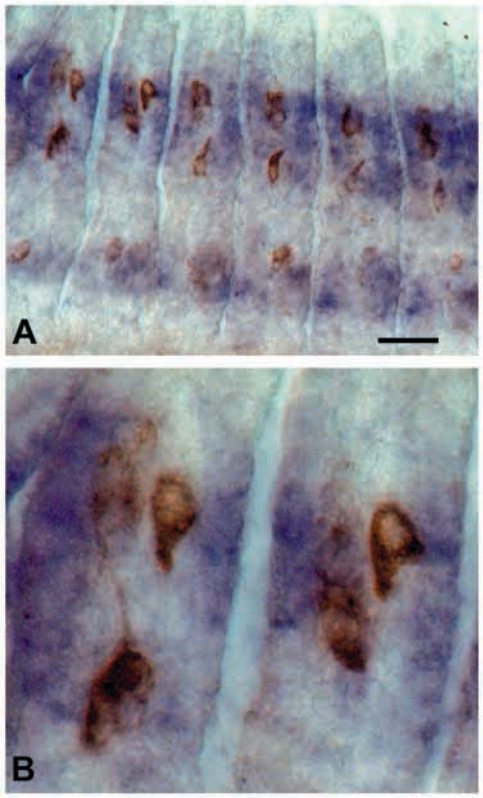

Fig. 6. *Tollo* mRNA is expressed in ectodermal cells that surround differentiating neurons. After in situ hybridization (purple), embryos were stained with mAb 22C10 (brown) to visualize the relationship between differentiating neurons and Tollo-expressing ectodermal cells. (A) Segments of the peripheral ectoderm are shown (T2-A4, anterior towards the left, dorsal towards the top of the panel) from an early stage 14 embryo. Neurons differentiate within domains of *tollo* mRNA expression. (B) Higher magnification of T2 and T3 from A shows the intimate relationship between Tollo-expressing ectodermal cells and differentiating neurons. Scale bar: 60 μm in A; 20 μm in B.

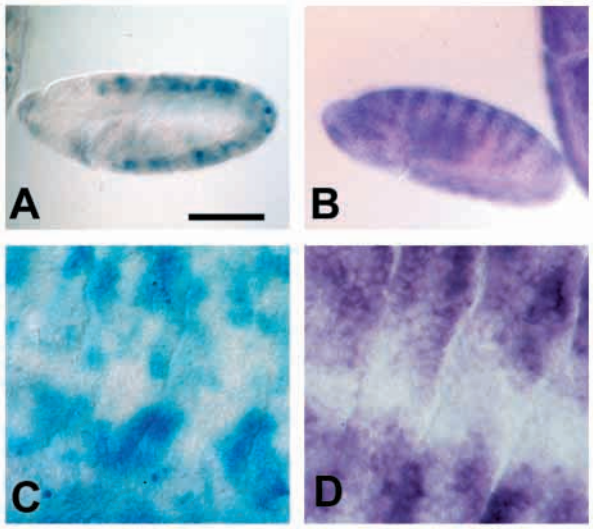

Fig. 7. A *tollo*-Gal4 transgene drives *lacZ* expression (from UAS-*lacZ*) in the same cells that express Tollo mRNA. (A,C) *lacZ* activity visualized in *tollo*-Gal4; UAS-*lacZ* embryos. (B,D) Tollo mRNA detected in OreR embryos by in situ hybridization. In stage 12, germ band-extended embryos (A,B), *lacZ* activity (A) is detected in segmentally repeated bands of ectodermal cells that mirror Tollo mRNA (B). In the peripheral ectoderm at stage 13 (C,D) *lacZ* activity (C) is detected in domains of ectodermal cells. Segments T3 – A2 are shown in C,D, anterior towards the left and dorsal towards the top of the panel. Scale bar: 350 μm in A,B; 60 μm in C,D.

DISCUSSION

Tollo induces neuron-specific glycosylation

Nearly a half-century of molecular biochemistry has documented tissue-specific, cell-specific, stage-specific, and disease-specific oligosaccharide presentation (Varki, 1993; Dennis et al., 1999; Lowe, 2001; Paulson and Colley, 1989; Amado et al., 1999). Despite this wealth of information, few descriptions exist of molecular mechanisms that control the specificity of glycan expression (Turkington et al., 1968; Rajput et al., 1996; Qian et al., 2001). Glycan synthesis has been modulated by manipulating various transmembrane signaling pathways, indicating that receptor-mediated events at the cell surface can influence oligosaccharide profiles (Carlow et al., 2001; Wagers and Kansas, 2000; Chen et al., 1998). Although the surface receptors that transmit these signals have not been identified, our results demonstrate that the Tollo/Toll-8 transmembrane protein influences cell-specific glycan expression in the *Drosophila* embryo.

The localization of Tollo expression to non-neural ectodermal cells and the rescue of neural-specific glycosylation by transgenic *tollo* both demonstrate that non-homologous cells modulate glycan expression in adjacent tissues. The close proximity of Tollo-expressing ectodermal cells to differentiating neurons is consistent with a molecular mechanism in which neural glycosylation is influenced by the activity of a neuronal surface receptor that directly binds ectodermal Tollo. Alternatively, the molecular activity of *tollo* may reside entirely within the ectodermal cell, exerting an indirect influence on neural glycosylation by propagating or attenuating instructive signals subsequently interpreted by local neurons. At present, our data cannot unambiguously distinguish whether the direct or indirect mechanism applies. However, the results of HRP-epitope rescue and Tollo misexpression studies indicate requirements that both models must satisfy.

Molecular mechanisms derived from Tollo expression, misexpression and HRP-epitope rescue

Neuronal synthesis of the HRP-glycan is rescued in Brd^{15}/Brd^{15} embryos when Tollo is expressed in its wild-type ectodermal pattern (*tollo*-Gal4/UAS-*tollo*). However, *ELAV*-

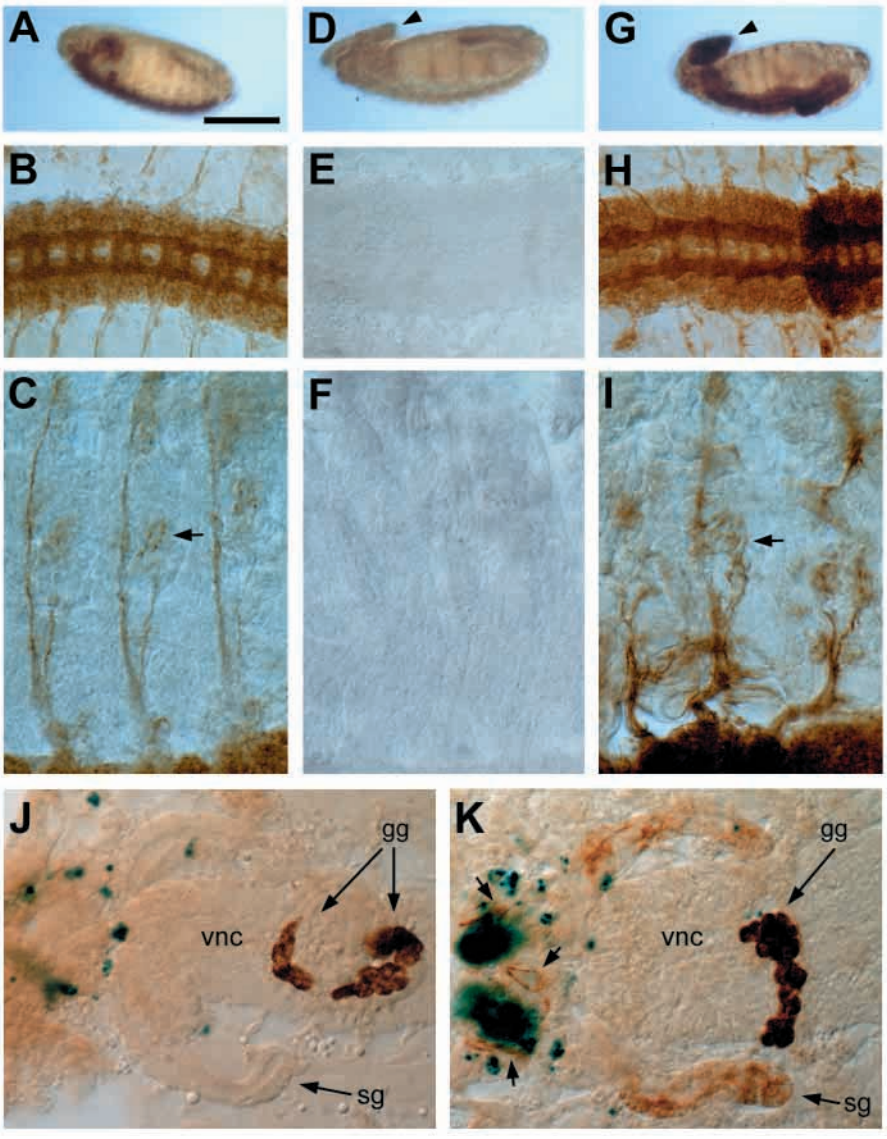

Fig. 8. Transgenic expression of Tollo in Brd^{15} homozygotes rescues expression of the HRP epitope in the ventral nerve cord and in the peripheral nervous system. All panels show embryos probed with anti-HRP antibody. Whole-mount (A,D,G), ventral nerve cord (B,E,H) and three segments (C,F,I) of the peripheral nervous system are shown in OreR (A-C, stage 15), Brd^{15}/Brd^{15} (D-F, stage 16) and *tollo*-Gal4; UAS-*tollo*; Brd^{15}/Brd^{15} (G-I, stage 16) embryos. Transgenic Tollo rescues expression of the HRP epitope in the ventral nerve cord (G,H) but does not correct the head involution defect associated with the Brd^{15} deletion (compare arrowheads in D and G). HRP-epitope expression in elements of the peripheral nervous system first becomes apparent at stage 15 in OreR (short arrow in C). Loss of the HRP epitope in the peripheral nervous system of Brd^{15} homozygotes (F) is rescued by Tollo (short arrow in I). Tollo expression under control of *hsp70*-Gal4 without heat shock (J,K) induces HRP-epitope expression in the salivary gland (sg, paired structures at top and bottom of J,K) and rescues epitope expression in nearby sensory neurons (short arrows in K). The anterior end of dissected *hsp70*-Gal4; UAS-*tollo*; Brd^{15}/TM3-*lacZ* embryos at stage 14 (J) and at stage 16 (K) are shown, anterior towards the left, after sequential *lacZ* activity staining (blue) and anti-HRP antibody staining. At dissection, the anterodorsal ectoderm of the head was sliced at the dorsal midline and flattened laterally. Subsequent removal of the embryonic brain lobes reveals the rescued sensory neurons (gg, garland gland; vnc, ventral nerve cord). Scale bar: 450 μm in A,D,G; 125 μm in B,E,H; 63 μm in C,F,I; 115 μm in J,K.

Gal4/UAS-*tollo* and *rho*-Gal4/UAS-*tollo* embryos fail to rescue the HRP epitope, despite driving misexpression in neurons and glia that would present Tollo to neuronal surfaces at developmental stages coincident with the normal Tollo expression pattern. Therefore, if *tollo* acts directly to alter neural glycosylation, ectodermal presentation of Tollo must be unique in comparison with expression in other cell types that also share contact with neurons; either the Tollo protein requires an ectodermal-specific post-translational modification for activity or an ectodermal co-factor is necessary for appropriate presentation to neurons. If *tollo* indirectly affects neural glycosylation by generating or influencing paracrine signals sensed by differentiating neurons, then the cellular context in which Tollo is expressed determines induction of the HRP epitope; either the relevant paracrine influence is specifically of ectodermal origin or a required *tollo* intracellular signaling pathway is absent from neurons and glia.

The indirect mechanism is consistent with the function of other TLRs (Belvin and Anderson, 1996; Cantera et al., 1999; Halfon and Keshishian, 1998) and is supported by two additional observations. First, the discontinuous distribution of *tollo* mRNA in the neurogenic ectoderm of the ventral nerve cord indicates that *tollo* expression is limited to ectodermal cells contacting only a subset of the total differentiating neuron pool. Therefore, global CNS expression of the HRP epitope requires a signal unrestricted by the need for cell-cell contact. Second, HRP-epitope expression is rescued in PNS sensory neurons located near salivary glands that ectopically express Tollo, consistent with the generation of a locally active signal. Expression of the HRP epitope is not rescued in the CNS nor in more remote parts of the PNS by *hsp70*-Gal4/UAS-*tollo*, implying that temporal and physical barriers can limit Tollo activity.

The unexpected, ectopic expression of the HRP epitope in the secretory epithelium of the salivary gland indicates that some developing tissues are only one signal away from assuming an altered glycosylation phenotype. At least within the salivary gland, this result also indicates that Tollo can act directly or can generate an autocrine signal that autonomously modulates glycosylation. For neural tissue, though, elaboration of the HRP epitope is a non-autonomous neuronal behavior that requires ectodermal Tollo expression. By analogy to Toll, soluble protein ligands (like Spätzle) are prime candidates for the Tollo activator, but the full diversity of TLR ligands has yet to be characterized in any organism (Hoffman et al., 1999; Yang et al., 1998; Belvin and Anderson, 1996).

The structure of the HRP epitope predicts downstream targets of Tollo signaling

In plants and in the *Drosophila* adult, HRP-epitope structure has been demonstrated to contain an extensively trimmed high-mannose core carrying an α3-linked Fuc residue on the internal GlcNAc of the chitobiose. (Fabini et al., 2001; Kurosaka et al., 1991). To generate the described *Drosophila* HRP epitopes, high-mannose oligosaccharides must first be trimmed to a $Man_3GlcNAc_2$ or $Man_2GlcNAc_2$ core. The core structure is then di-fucosylated (α3 and α6), requiring the activity of two distinct fucosyltransferases. Addition of Fuc α3 to the core requires previous and transient addition of GlcNAc to a terminal Man, yielding a di-fucosylated $Man_{2/3}GlcNAc_2$ oligosaccharide (Fabini et al., 2001; Altmann et al., 1993; Altmann et al., 1995). Therefore, trimming mannosidases, two fucosyltransferases, an N-acetylglucosaminyltransferase and a hexosaminidase constitute the minimal set of processing activities required to generate an HRP epitope. Of these activities, addition of the α3 Fuc imparts antibody recognition to the oligosaccharide.

A *Drosophila* fucosyltransferase that adds Fuc in α3 linkage to core GlcNAc has been characterized (Fabini et al., 2001). Designated 'FucTA', the enzyme exhibits in vitro acceptor specificity appropriate for synthesis of the HRP epitope and the gene maps to 71B2, 87 kb distal to *tollo*. Although this lies within the Brd^{15} deletion, combining *tollo*-Gal4 with UAS-*tollo* results in rescue of HRP epitope expression in Brd^{15} homozygotes. Therefore, glycan expression is rescued by Tollo/Toll-8 in a *FucTA* null background. The relevance of FucTA activity to HRP-epitope expression in the embryonic nervous system remains to be determined, but *Drosophila* requires α3 fucosyltransferase activity and the resulting capacity to synthesize the HRP epitope in multiple contexts. Mutants that lack the HRP epitope in larval and adult stages express the oligosaccharide embryonically and epitope expression in embryonic non-neural tissue is maintained in mutants that lack the embryonic neural oligosaccharide (Snow et al., 1987; Katz et al., 1988). Thus, multiple pathways, under independent control and active in different tissues and developmental stages, lead to synthesis of the HRP epitope.

An oligosaccharide of unknown function reveals a new function for Toll-like receptors

Our results suggest superficially that loss of the HRP epitope is of relatively little consequence. However, the component of the HRP epitope structure that imparts antibody recognition may be distinct from the functional domain of the oligosaccharide. Therefore, mutations in genes such as *tollo*, which affect specific carbohydrate expression, may not immediately reveal oligosaccharide function. The *nac* mutant, which lacks larval, pupal and adult expression of the HRP epitope, exhibits grossly normal nervous system morphology (Katz et al., 1988; Phillis et al., 1993). Highly penetrant axon defasciculation errors are present in the *nac* adult but only become apparent when afferent projections arising from discrete subsets of dye-labeled sensory neurons in the wing margin are visualized at their entry point into the central nervous system (Whitlock, 1993). Until techniques of similar resolution are applied to embryos that lack the HRP epitope, the functional significance of loss of this tissue-specific glycan cannot be fully evaluated.

In *Drosophila*, the HRP epitope is present on several neural proteins, many of which are also expressed in non-neural tissue where they lack the glycan (Desai et al., 1994; Snow et al., 1987; Sun et al., 1995; Wang et al., 1994). Thus, cells determine whether or not to construct the HRP epitope on a particular glycoprotein based on the tissue in which the protein is expressed, rather than on a signal intrinsic to the polypeptide. While *tollo*/*toll-8* demonstrates that such tissue-specific glycan expression can be achieved through the activity of a Toll-like receptor, the correlation between *Drosophila* TLR expression and specific glycosylation patterns cannot be comprehensively assessed before glycan characterization in the *Drosophila* embryo is greatly expanded (Fabini et al., 2001; Seppo and Tiemeyer, 2000). Nonetheless, distributions of other TLRs

exhibit spatial and temporal overlap with Tollo expression, raising the possibility that TLRs sculpt embryonic glycosylation patterns through combinatorial activation of glycosylation pathways in interacting domains of developing tissues (Hashimoto et al., 1988; Eldon et al., 1994; Chiang and Beachy, 1994; Stathopolous and Levine, 2002).

TLRs mediate pattern recognition (frequently glycan-based) as part of the innate, non-adaptive immune response in *Drosophila* and vertebrates (Hoffman et al., 1999; Medzhitov et al., 1997; Williams et al., 1997; Yang et al., 1998). However, only a subset of *Drosophila* TLRs induce defensive responses. TLR family members appear divided into clans that function in innate immunity or that fulfill developmental needs (Tauszig et al., 2000). The capacity to control glycosylation could unite the TLR family in support of a common cause, to produce appropriate spatial and temporal patterns of cell-specific glycosylation. Expressed by immune cell types that participate in tissue surveillance, TLRs are positioned to locally influence cellular glycosylation in response to pathogen, thereby coupling innate detection of non-self patterns with expression of protective glycans on host cells. In addition, further analysis of the distribution and function of TLRs may indicate that the constitutive maintenance of diverse tissue glycan profiles is generally an active process in which glycan expression is continually renewed or responsively modified by TLR-mediated signaling. In mature tissues and in the embryo, the expression of glycans must be orchestrated to coincide with the appearance of relevant carbohydrate binding proteins that mediate cell adhesion and recognition (Varki, 1993; Sharrow and Tiemeyer, 2001; Feinberg et al., 2001; Song and Zipser, 1995; Vyas et al., 2002). Therefore, broader mechanisms that impart specificity to cell-cell interactions are likely to be revealed with further characterization of the pathway by which *tollo/toll-8* controls oligosaccharide expression.

The authors are indebted to Marc Schwartz, Reed Kelso and Jay Goodman for deletion mapping; Corey Goodman for supplying antibodies; and Carl Hashimoto, Lynn Cooley and members of their respective laboratories for advice. Digital image acquisition was expertly facilitated by Peter Tiemeyer. Grant support from the NIH-NICD (HD33878), from the March of Dimes (Basil O'Connor Award), and from the Patrick and Catherine Weldon Donaghue Foundation is gratefully acknowledged. M. S. and P. M. received support from NIH-NIGMS (GM07223). A. S. was funded by the Finnish Academy and by a Postdoctoral Fellowship from the HFSPO.

REFERENCES

Adams, M. D., Celniker, S. E., Holt, R. A., Evans, C. A., Gocayne, J. D., Amanatides, P. G., Scherer, S. E., Li, P. W., Hoskins, R. A., Galle, R. F. et al. (2000). The genome sequence of *Drosophila melanogaster*. *Science* **287**, 2185-2195.

Allendoerfer, K. L., Durairaj, A., Matthews, G. A. and Patterson, P. H. (1999). Morphological domains of Lewis-X/FORSE-1 immunolabeling in the embryonic neural tube are due to developmental regulation of cell surface carbohydrate expression. *Dev. Biol.* **211**, 208-219.

Altmann, F., Kornfeld, G., Dalik, T., Staudacher, E. and Glossl, J. (1993). Processing of asparagine-linked oligosaccharides in insect cells. N-acetylglucosaminyltransferase I and II activities in cultured lepidopteran cells. *Glycobiology* **3**, 619-625.

Altmann, F., Schwihla, H., Staudacher, E., Glossl, J. and Marz, L. (1995). Insect cells contain an unusual, membrane-bound beta-N-acetylglucosaminidase probably involved in the processing of protein N-glycans. *J. Biol. Chem.* **270**, 17344-17349.

Altschul, S. F., Madden, T. L., Schäffer, A. A., Zhang, J., Zhang, Z., Miller, W. and Lipman, D. J. (1997). Gapped BLAST and PSI-BLAST: a new generation of protein database search programs. *Nucleic Acids Res.* **25**, 3389-3402.

Amado, M., Almeida, R., Schwientek, T. and Clausen, H. (1999). Identification and characterization of large galactosyltranferase gene families: galactosyltransferases for all functions. *Biochim. Biophys. Acta* **1473**, 35-53.

Anderson, K. V., Jürgens, G. and Nüsslein-Volhard, C. (1985). Establishment of dorsal-ventral polarity in the *Drosophila* embryo: genetic studies on the role of the *Toll* gene product. *Cell* **42**, 779-789.

Belvin, M. P. and Anderson, K. V. (1996). A conserved signaling pathway: The *Drosophila* Toll-Dorsal Pathway. *Ann. Rev. Cell Dev. Biol.* **12**, 393-416.

Blochinger, K., Jan, L. Y. and Jan, Y. N. (1990). Patterns of expression of Cut, a protein required for external sensory organ development, in wild-type and *cut* mutant *Drosophila* embryos. *Genes Dev.* **4**, 1322-1331.

Brand, A. H. and Perrimon, N. (1993). Targeted gene expression as a means of altering cell fates and generating dominant phenotypes. *Development* **118**, 401-415.

Brand, A. H., Manoukian, A. S. and Perrimon, N. (1994). Ectopic Expression in *Drosophila*. In Drosophila melanogaster*: Practical Uses in Cell and Molecular Biology*, Vol. 44 (ed. L. S. B. Goldstein and E. Fyrberg), pp. 635-654. San Diego, CA: Academic Press.

Campos-Ortega, J. A. and Hartenstein, V. (1985). In *The Embryonic Development of* Drosophila melanogaster, pp. 3-84. Berlin: Springer-Verlag.

Cantera, R., Kozlova, T., Barillas-Mury, C. and Kafatos, F. C. (1999). Muscle structure and innervation are affected by loss of Dorsal in the fruit fly, *Drosophila melanogaster*. *Mol. Cell. Neurosci.* **13**, 131-141.

Carlow, D. A., Corbel, S. Y., Williams, M. J. and Ziltener, H. J. (2001). IL-2, -4, and -15 differentially regulate O-glycan branching and P-selectin ligand formation in activated CD8 T cells. *J. Immunol.* **167**, 6841-6848.

Chen, L., Zhang, W., Fregien, N. and Pierce, M. (1998). The her-2/neu oncogene stimulates the transcription of N-acetylglucosaminyltransferase V and expression of its cell surface oligosaccharide products. *Oncogene* **17**, 2087-2093.

Chiang, C. and Beachy, P. A. (1994). Expression of a novel *Toll*-like gene spans the parasegment boundary and contributes to *hedgehog* function in the adult eye of *Drosophila*. *Mech. Dev.* **47**, 225-239.

Dennis, J. W., Granovsky, M. and Warren, C. E. (1999). Glycoprotein glycosylation and cancer progression. *Biochim. Biophys. Acta* **1473**, 21-34.

Desai, C. J., Popova, E. and Zinn, K. (1994). A *Drosophila* receptor tyrosine phosphatase expressed in the embryonic CNS and larval optic lobes is a member of the set of proteins bearing the 'HRP' carbohydrate epitope. *J. Neurosci.* **14**, 7272-7283.

Dodd, J. and Jessell, T. W. (1985). Lactoseries carbohydrates specify subsets of dorsal root ganglion neurons projecting to the superficial dorsal horn of rat spinal cord. *J. Neurosci.* **5**, 3278-3294.

Eldon, E., Kooyer, S., D'Evelyn, D., Duman, M., Lawinger, P., Botas, J. and Bellen, H. (1994). The *Drosophila* 18-wheeler is required for morphogenesis and has striking similarities to Toll. *Development* **120**, 885-899.

Fabini, G., Freilinger, A., Altmann, F. and Wilson, I. B. (2001). Identification of core alpha 1,3-fucosylated glycans and cloning of the requisite fucosyltransferase cDNA from *Drosophila melanogaster*. Potential basis of the neural anti-horseradish peroxidase epitope. *J. Biol. Chem.* **276**, 28058-28067.

Feinberg, H., Mitchell, D. A., Drickamer, K. and Weis, W. I. (2001). Structural basis for selective recognition of oligosaccharides by DC-SIGN and DC-SIGNR. *Science* **294**, 2163-2166.

Feizi, T. (1985). Demonstration by monoclonal antibodies that carbohydrate structures of glycoproteins and glycolipids are onco-developmental antigens. *Nature* **314**, 53-57.

Frohman, M. (1993). Rapid amplification of complementary DNA ends for generation of full-length complementary DNAs: thermal RACE. *Met. Enzymol.* **218**, 340-356.

Halfon, M. S. and Keshishian, H. (1998). The Toll pathway is required in the epidermis for muscle development in the *Drosophila* embryo. *Dev. Biol.* **199**, 164-174.

Hammond, C., Braakman, I. and Helenius, A. (1994). Role of N-linked oligosaccharide recognition, glucose trimming, and calnexin in glycoprotein folding and quality control. *Proc. Natl. Acad. Sci.* **91**, 913-917.

Hashimoto, C., Hudson, K. L. and Anderson, K. V. (1988). The *Toll* gene of *Drosophila*, required for dorsal-ventral embryonic polarity, appears to encode a transmembrane protein. *Cell* **52,** 269-279.

Hoffman, J. A., Kafatos, F. C., Janeway, C. A. and Ezekowitz, R. A. (1999). Phylogenetic perspectives in innate immunity. *Science* **284**, 1313-1318.

Ip, Y. T. and Levine, M. (1994). Molecular genetics of *Drosophila* immunity. *Curr. Opin. Genet. Dev.* **4**, 672-677.

Jan, L. Y. and Jan, Y. N. (1982). Antibodies to horseradish peroxidase as specific neuronal markers in *Drosophila* and grasshopper embryos. *Proc. Natl. Acad. Sci. USA* **79**, 2700-2704.

Katz, F., Moats, W. and Jan, Y. N. (1988). A carbohydrate epitope expressed uniquely on the cell surface of *Drosophila* neurons is altered in the mutant *nac* (neurally altered carbohydrate). *EMBO J.* **7**, 3471-3477.

Klämbt, C., Jacobs, J. R. and Goodman, C. S. (1991). The midline of the *Drosophila* central nervous system: a model for the genetic analysis of cell fate, cell migration, and growth cone guidance. *Cell* **64**, 801-815.

Kopczynski, C. C., Davis, G. W. and Goodman, C. S. (1996). A neural tetraspanin, encoded by *late bloomer*, that facilitates synapse formation. *Science* **271**, 1867-1870.

Kurosaka, A., Yano, A., Itoh, N., Kuroda, Y., Nakagawa, T. and Kawasaki, T. (1991). The structure of a neural specific carbohydrate epitope of horseradish peroxidase recognized by anti-horseradish peroxidase antiserum. *J. Biol. Chem.* **266**, 4168-4172.

Leviten, M. W. and Posakony, J. W. (1996). Gain-of-function alleles of *Bearded* interfere with alternative cell fate decisions in *Drosophila* adult sensory organ development. *Dev. Biol.* **176**, 264-283.

Lindsley, D. L. and Zimm, G. G. (1992). In *The Genome of* Drosophila melanogaster, p. 1075. San Diego, CA: Academic Press.

Lowe, J. B. (2001). Glycosylation, immunity, and autoimmunity. *Cell* **104**, 809-812.

Matthews, R. T., Kelly, G. M., Zerillo, C. A., Tiemeyer, M. and Hockfield, S. (2002). Aggrecan glycoforms contribute to the molecular heterogeneity of perineuronal nets. *J. Neurosci.* **22**, 7536-7547.

Medzhitov, R., Preston-Hurlburt, P. and Janeway, C. A. (1997). A human homologue of the *Drosophila* Toll protein signals activation of adaptive immunity. *Nature* **388**, 394-397.

Moloney, D. J., Panin, V. M., Johnston, S. H., Chen, J., Shao, L., Wilson, R., Wang, Y., Stanley, P., Irvine, K. D., Haltiwanger, R. S. and Vogt, T. F. (2000). Fringe is a glycosyltransferase that modifies Notch. *Nature* **406**, 357-358.

Patel, N. H. (1994). Imaging neuronal subsets and other cell types in whole mount *Drosophila* embryos and larvae using antibody probes. In Drosophila melanogaster*: Practical Uses in Cell and Molecular Biology*, Vol. 44 (ed. L. S. B. Goldstein and E. Fyrberg), pp. 445-487. San Diego, CA: Academic Press.

Paulson, J. C. and Colley, K. J. (1989). Glycosyltransferases: structure, localization and control of cell type-specific glycosylation. *J. Biol. Chem.* **264**, 17615-17618.

Phillis, R. W., Bramlage, A. T., Wotus, C., Whittaker, A., Gramates, L. S., Seppala, D., Farahanchi, F., Caruccio, P. and Murphey, R. K. (1993). Isolation of mutations affecting neural circuitry required for grooming behavior in *Drosophila melanogaster*. *Genetics* **133**, 581-592.

Qian, R., Chen, C. and Colley, K. J. (2001). Location and mechanism of alpha2,6-sialyltransferase dimer formation. Role of cysteine residues in enzyme dimerization, localization, activity and processing. *J. Biol. Chem.* **276**, 28641-28649.

Rajput, B., Shaper, N. L. and Shaper, J. H. (1996). Transcriptional regulation of murine beta1,4-galactosyltransferase in somatic cells. Analysis of a gene that serves both a housekeeping and a mammary gland-specific function. *J. Biol. Chem.* **271**, 5131-5142.

Rubin, G. M., Hong, L., Brokstein, P., Evans-Holm, M., Frise, E., Stapleton, M. and Harvey, D. A. (2000). A Drosophila complementary DNA resource. *Science* **287**, 2222-2224.

Sambrook, J., Fritsch, E. and Maniatis, T. (1989). In *Molecular Cloning: A Laboratory Manual*. Plainview, NY: Cold Spring Harbor Laboratory Press.

Seppo, A. and Tiemeyer, M. (2000). Function and structure of *Drosophila* glycans. *Glycobiology* **10**, 751-760.

Sharrow, M. and Tiemeyer, M. (2001). Gliolectin-mediated carbohydrate binding at the *Drosophila* midline ensures the fidelity of axon pathfinding. *Development* **128**, 4585-4595.

Snow, P. M., Patel, N. H., Harrelson, A. L. and Goodman, C. S. (1987). Neural-specific carbohydrate moiety shared by many surface glycoproteins in *Drosophila* and grasshopper embryos. *J. Neurosci.* **7**, 4137-4144.

Song, J. and Zipser, B. (1995). Targeting of neuronal subsets mediated by their sequentially expressed carbohydrate markers. *Neuron* **14**, 537-547.

Stathopoulus, A. and Levine, M. (2002). Dorsal gradient networks in the *Drosophila* embryo. *Dev. Biol.* **246**, 57-67.

Sun, B. and Salvaterra, P. M. (1995) Characterization of Nervana, a *Drosophila melanogaster* neuron-specific glycoprotein antigen recognized by anti-horseradish peroxidase antibodies. *J. Neurochem.* **65**, 434-443.

Tauszig, S., Jouanguy, E., Hoffman, J. A. and Imler, J. L. (2000). Toll-related receptors and the control of antimicrobial peptide expression in *Drosophila*. *Proc. Natl. Acad. Sci. USA* **97**, 10520-10525.

Tautz, D. and Pfeifle, C. (1989). A non-radioactive in situ hybridization method for the localization of specific RNAs in *Drosophila* embryos reveals translational control of the segmentation gene *hunchback*. *Chromosoma* **98**, 81-85.

Tsuda, M., Kamimura, K., Nakato, H., Archer, M., Staatz, W., Fox, B., Humphrey, M., Olson, S., Futch, T., Kaluz, V., Siegfried, E., Stam, L. and Selleck, S. B. (1999). The cell-surface proteoglycan Dally regulates Wingless signaling in *Drosophila*. *Nature* **400**, 276-280.

Turkington, R. W., Brew, K., Vanaman, T. C. and Hill, R. L. (1968). The hormonal control of lactose synthetase in the developing mouse mammary gland. *J. Biol. Chem.* **243**, 3382-3387.

Varki, A. (1993). Biological roles of oligosaccharides. *Glycobiology* **3**, 97-130.

Vyas, A. A., Patel, H. V., Fromholt, S. E., Heffer-Lauc, M., Vyas, K. A., Dang, J., Schachner, M. and Schnaar, R. L. (2002). Gangliosides are functional nerve cell ligands for myelin-associated glycoprotein (MAG), an inhibitor of nerve regeneration. *Proc. Natl. Acad. Sci. USA* **99**, 8412-8417.

Wagers, A. J. and Kansas, G. S. (2000). Potent induction of alpha(1,3)-fucosyltransferase VII in activated CD4+ T cells by TGF-beta 1 through a p38 mitogen-activated protein kinase-dependent pathway. *J. Immunol.* **165**, 5011-5016.

Wang, X., Sun, B., Yasuyama, K. and Salvaterra, P. M. (1994). Biochemical analysis of proteins recognized by anti-HRP antibodies in *Drosophila melanogaster*: identification and characterization of neuron specific and male specific glycoproteins. *Insect Biochem. Mol. Biol.* **24**, 233-242.

Whitlock, K. E. (1993). Development of *Drosophila* wing sensory neurons in mutants with missing or modified cell surface molecules. *Development* **117,** 1251-1260.

Williams, M. J., Rodriguez, A., Kimbrell, D. A. and Eldon, E. D. (1997). The *18-wheeler* mutation reveals complex antibacterial gene regulation in *Drosophila* host defense. *EMBO J.* **16**, 6120-6130.

Yang, R. B., Mark, M. R., Gray, A., Huang, A., Xie, M. H., Zhang, M., Goddard, A., Wood, W. I., Gurney, A. L. and Godowski, P. J. (1998). Toll-like receptor-2 mediates lipopolysaccharide-induced cellular signalling. *Nature* **395**, 284-288.

Yuki, S., Inouye, S., Ishimaru, S. and Saigo, K. (1986). Nucleotide sequence characterization of a *Drosophila* retrotransposon. *Eur. J. Biochem.* **158**, 403-410.